MAGNETIC SUSPENSION OF FLEXIBLE STRUCTURES FOR NON-CONTACT PROCESSING

Ming-chih Weng
Seagate Technologies, Costa Mesa, CA, USA, mingchih@alum.mit.edu
Xiaodong Lu
Massachusetts Institute of Technology, Cambridge, MA, USA, xdlu@mit.edu
David L. Trumper
Massachusetts Institute of Technology, Cambridge, MA, USA, trumper@mit.edu

ABSTRACT
This paper presents the magnetic suspension of elongated workpieces by using multiple electromagnetic actuators and multiple position sensors. Our particular focus is on the use of such suspensions in manufacturing processes such as coating and painting which can be facilitated by non-contact handling. We have developed a novel approach for the control of such non-contact suspensions through what we term **sensor averaging** and **actuator averaging**. The difficult stability and robustness problems imposed by the flexible dynamics of the workpiece can be overcome by taking a properly-weighted average of the outputs of a distributed array of *N* motion sensors (sensor averaging), and/or by applying a properly-weighted distributed array of *M* forces (actuator averaging) to the workpiece. The theory for these dual techniques is developed in detail in the paper. These approaches are shown to be independent of the specific boundary conditions or the longitudinal dimensions of the workpiece. We experimentally demonstrate the utility of our theory in the successful magnetic suspension of a 3 m long, 6.35 mm diameter, 0.89 mm wall thickness steel tube with varying boundary conditions. This suspension uses 8 two-degree-of-freedom actuators and 8 two-degree-of-freedom sensors distributed along the length of the workpiece.

INTRODUCTION
The ability of suspending workpieces without contact can facilitate various manufacturing processes, such as coating, painting, heat treating, and web handling [1,2,3]. The suspended objects may have varying boundary conditions, varying structure lengths, and varying structure positions. It is very challenging to robustly stabilize such a time-varying system. Furthermore, it is generally difficult to control the structural vibration since: (1) The structures may have extremely light damping. (2) At high frequencies, we have significant phase lag from sensor dynamics, actuator dynamics, and time delay from the digital controller. (3) The paired sensor and actuator can not be physically collocated. When some resonance nodes fall in between the paired sensor and actuator, this non-collocation problem causes the control effort to be out of phase by 180^o for these modes, and can destabilize the system.

We stabilize the structural vibration in two ways: (1) At low frequencies, we want to add damping to the resonance modes by using a lead compensator. (2) At high frequencies, we want to reduce the gains of the resonance modes without adversely affecting the phase, which is practically very difficult to accomplish. The following methods are frequently considered to stabilize the resonance modes at high frequencies:

1. Add a lead compensator to high frequencies: The disadvantage is that this also amplifies the gains of the modes at higher frequencies, and these higher frequency modes can destabilize the system.
2. Add a low-pass filter to high frequencies: This method introduces phase lag to the modes at lower frequencies, and these lower frequency modes can then destabilize the system.
3. Reduce the controller gain: This is undesirable since it reduces the suspension stiffness.
4. Design notch filters to exactly cancel the modes: This is essentially a model-based controller. A change of boundary conditions or structural lengths can easily destabilize such a system.
5. Place sensors or actuators on the nodes of the corresponding unstable modal shapes: This is also a model-based method, and is sensitive to system uncertainties and changes.

In this paper, we present our **sensor averaging** and **actuator averaging** methods to solve this stability problem. Both methods can robustly attenuate the gains of undesired resonance modes without adversely

affecting the phase. These methods are a new concept for a non-model-based modal-band-stop filter. We use the suspension of a tubular beam to demonstrate these two methods; this system is shown in Fig. 1.

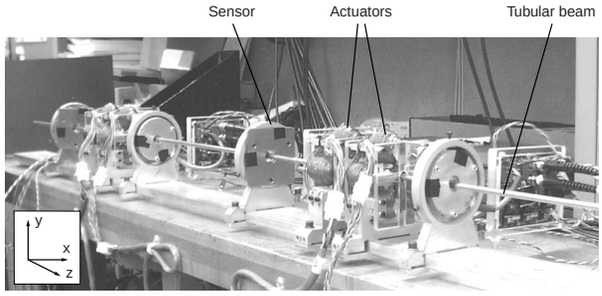

FIGURE 1: Experimental setup: magnetic suspension of a tubular beam.

SENSOR/ACTUATOR AVERAGING

The simplest arrangement for sensor averaging places 2 sensors set apart by a distance of $2d_s$, and uses the averaged measurement as a single output for feedback. Hence the resonance modes with wavelengths close to $4d_s$ will have opposite deflections at the 2 sensors, and thus a low contribution to the averaged output. Actuator averaging is the dual to sensor averaging. Here, two actuators are spaced apart by a distance of $2d_a$, and we apply the same force to each actuator. Since the modes will be forced in opposite directions if their wavelength is close to $4d_a$, this results in a similar nulling effect. On this basis, we show that sensor/actuator averaging can reduce modal observability/controllability over a broad range of undesired resonance modes without adversely affecting the measurement or actuation phase. Another advantage of using these averaging methods is that they only depend on the properties of the structure element, and are independent of boundary conditions, structure lengths, or structure positions.

SENSOR AVERAGING FOR BEAMS

We use the average of multiple sensors' measurements to stand for a single point's displacement. Fig. 2 shows the different arrangements of sensor locations that we will study in the following sections, including 2-sensor averaging, 3-sensor averaging, and with more general sensor weightings.

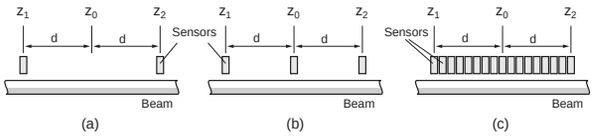

FIGURE 2: Sensor positioning for beams: (a) 2 sensors, (b) 3 sensors, (c) many sensors.

Dynamic Analyses of Beams

We briefly review the structural dynamics of slender beams with negligible tension and negligible axial velocity. Details of this standard theory can be found in [4]. The beam equation can be written as

$$EI\frac{\partial^4 u}{\partial z^4}+\rho A\frac{\partial^2 u}{\partial t^2}=f \tag{1}$$

where EI is bending stiffness, z is axial coordinate, u is transverse deflection, ρ is material density, A is cross-sectional area, and f is an external transverse force density. The associated dispersion equation is

$$EIk_n^4=\rho A\omega_n^2 \tag{2}$$

where k_n is the wavenumber, and ω_n is the resonance frequency. The natural response of this beam equation can be represented by

$$u(z,t)=\sum_{n=1}^{\infty}\xi_n(t)\phi_n(z)$$

$$=\sum_{n=1}^{\infty}\xi_n(t)\left(C_{n1}\cos k_n z+C_{n2}\sin k_n z+C_{n3}e^{k_n z}+C_{n4}e^{-k_n z}\right) \tag{3}$$

where ξ_n is the nth modal coordinate, and ϕ_n is the nth modal shape. Here C_{n1} and C_{n2} represent sinusoidal waveforms with wavelengths $2\pi k_n$, and C_{n3} and C_{n4} represent evanescent waveforms that decay exponentially with increasing distances from the boundaries. The evanescent waveforms have negligible effects far away from the boundaries at high frequencies where k_n is large.

From modal analysis, the system dynamics can be decoupled into ordinary differential equations for each mode. The frequency response of the nth mode of beam dynamics can be represented as

$$\frac{\xi_n}{N_n}=\frac{1}{M_n\left(s^2+2\zeta_n\omega_n s+\omega_n^2\right)} \tag{4}$$

where N_n is modal force, M_n is modal mass, and ζ_n is modal damping ratio. If we have a point force input at z_a: $f(z,t)=f(t)\delta(z-z_a)$, and a position feedback at z_s: $y(t)=u(z_s,t)$, the frequency response from input f to output y becomes

$$\frac{y(s)}{f(s)}=\sum_{n=1}^{\infty}\frac{\phi_n(z_s)\phi_n(z_a)}{M_n\left(s^2+2\zeta_n\omega_n s+\omega_n^2\right)} \tag{5}$$

The modal shape at the sensor position z_s determines the modal observability $\phi_n(z_s)$, and the modal shape at the actuator position z_a determines the modal controllability $\phi_n(z_a)$. Eq. 5 suggests that the modal properties can be modified by sensor/actuator positioning.

2-Sensor Averaging

As shown in Fig. 2(a), we place 2 sensors set apart by a distance of $2d$, and use this average to represent the

displacement of the center point at $z=z_0$. The real displacement at z_0 is:

$$u(z_0,t)=\sum_{n=1}^{\infty}\xi_n(t)\phi_n(z_0) \quad (6)$$

and the averaged output from 2 sensors at $z_1=(z_0-d)$ and $z_2=(z_0+d)$ is:

$$\hat{u}(z_0,t)=0.5\left(u(z_1,t)+u(z_2,t)\right)$$

$$=0.5\sum_{n=1}^{\infty}\xi_n(t)\left(\phi_n(z_1)+\phi_n(z_2)\right)\approx\sum_{n=1}^{\infty}\xi_n(t)\phi_n(z_0)\cos k_n d \quad (7)$$

Eq. 7 neglects the exponential terms of the modal shape, since we assume we are far from the tube boundaries. Compare Eq. 6 and Eq. 7, each mode is multiplied by a modal gain of $\cos k_n d$ by using sensor averaging. Replacing the wavenumber k_n by frequency ω_n from the beam dispersion equation, the modal gain $\cos k_n d$ becomes

$$\cos k_n d=\cos\sqrt[4]{\frac{\rho A\omega_n^2}{EI}}d \quad (8)$$

Using our experimental setup as an example, the tubular beam has $(\rho A)/(EI)=0.01$. For a spacing $d=0.15$ m, the result of Eq. 8 is illustrated in Fig. 3. If we plot the modal gain as a function of wavenumber k_n, it is simply a cosine function. The notch zero is located at $k_n d=\pi/2$. When we plot the modal gain as a function of resonance frequency ω_n, the resulting plot shows that some resonance modes are attenuated near the notch zero at $\omega_n\approx1000$ rad/s. The phase stays unchanged before the notch, and flips by 180° after the notch when $\cos k_n d<0$. This result suggests that **by adjusting the sensor distance 2*d*, we can attenuate undesired resonance modes without adversely affecting the phase below the notch**. Furthermore, at frequencies below the cosine notch, all the resonance modes are in phase, which means there will be no sensor/actuator non-collocation problems for these modes.

To demonstrate this cosine effect on beam dynamics, we model the beam dynamics with an output $y(t)=(u(z_1,t)+u(z_2,t))/2$ instead of $y(t)=u(z_0,t)$. The resulting Bode plots is shown in Fig. 4, which includes the response of the evanescent waveforms. The modal gain $\cos k_n d$ creates an ideal band-stop filter for the resonance modes over a broad range of frequencies without adversely affecting the phase.

Modal Analysis of 2-Sensor Averaging

To further understand the behavior of sensor averaging, we can rewrite Eq. 7 by modal analysis, and it becomes

$$\frac{\hat{u}(s)}{f(s)}=\sum_{n=1}^{\infty}\left(\frac{\phi_n^2(z_0)}{M_n\left(s^2+2\zeta_n\omega_n s+\omega_n^2\right)}\cdot\cos k_n d\right) \quad (9)$$

In summary, 2-sensor averaging method has the following properties:

1. A waveform with wavelength 4*d* is unobservable.
2. It robustly attenuates the modal observability of waveforms with wavelengths close to 4*d*.
3. It is independent of sensor pair location z_0.

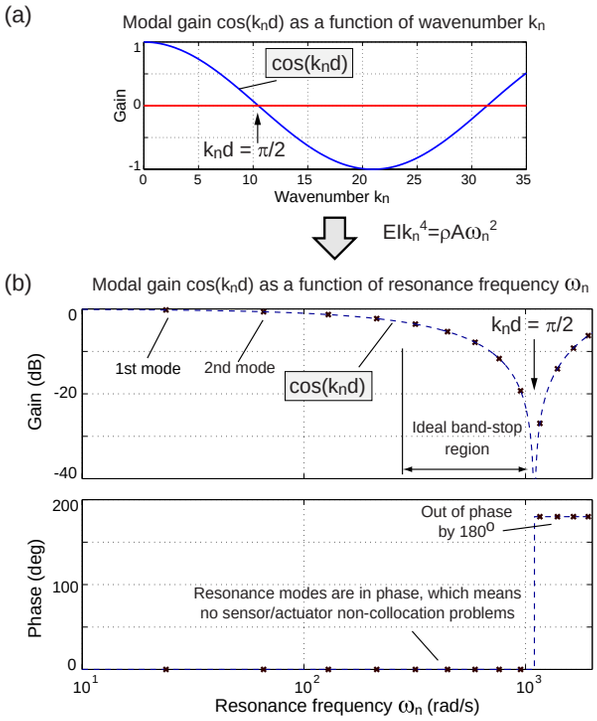

FIGURE 3: 2-Sensor averaging for beams: modal gain $\cos k_n d$ plotted as (a) a function of k_n, and (b) a function of ω_n.

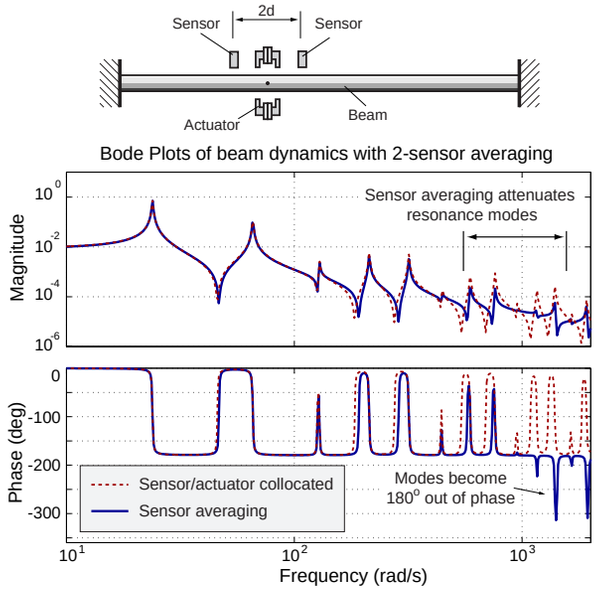

FIGURE 4: Theoretical beam model: Solid line shows a beam model with 2-sensor averaging, and a broad range of resonance modes are attenuated. Dashed line shows a beam model with collocated sensor and actuator.

4. It is independent of beam length and boundary conditions.
5. It eliminates possible non-collocation problems.
6. Sensor averaging causes no phase lag because it is a spatial filter, not a temporal filter. (Such spatial filter concepts have also been used in structural control via Discrete Modal Filters [5] and Distributed Sensors [6].)

3-Sensor Averaging

The sensor averaging method can be readily extended to more than 2 sensors. Using 3 sensors as shown in Fig. 2(b), and taking the averaged measurement as

$$\hat{u}(z_0,t) = 0.25u(z_1,t) + 0.5u(z_0,t) + 0.25u(z_2,t)$$
$$= \sum_{n=1}^{\infty}\left(\xi_n(t)\phi_n(z_0)\cdot\frac{1+\cos k_n d}{2}\right) \qquad (10)$$

gives a broader notch as shown in Fig. 5. The modal gain of $0.5(1+\cos k_n d)$ is always positive, and hence the 180° phase flip of 2-sensor averaging will not happen in 3-sensor averaging. The notch zero is now located at $k_n d=\pi$. Again using our experimental setup as an example, with d=0.30 m to have the notch near 1000 rad/s gives the results shown in Fig. 5.

The advantage of using 3 sensors is that phase remains zero for all frequencies, and the notch is broader than for 2-sensor averaging. The disadvantage is that the total sensor spacing $2d$ will be twice as long as for the two sensor case, if the notches are to be placed at the same frequency. This means that the sensor array will occupy a larger space on the workpiece.

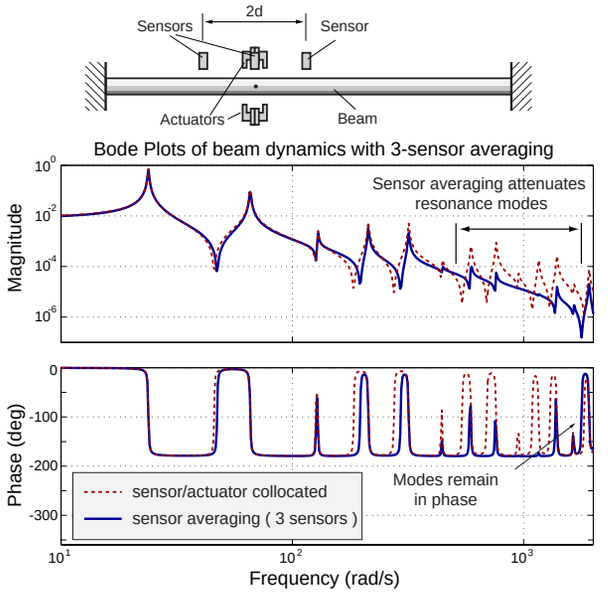

FIGURE 5: Theoretical beam model: Solid line shows 3-sensor averaging. Dashed line shows a collocated beam model.

Continuous-Sensor Averaging

The logical extension of the sensor averaging at 2 or 3 points is to use more sensors, as shown in Fig. 2(c). From the previous derivation, we realize that sensor averaging is a spatial filter, and is a dual to a temporal filter. Therefore we can adopt the theory for discrete-time finite-impulse-response (FIR) filters and apply it to sensor averaging. For example, by using 9 sensors with the weighting of a Blackman window, the resulting beam model is shown in Fig. 6. With this filter, the high frequency modes become almost unobservable. Resonance modes at even higher frequencies start to appear, with the interpretation that the wavelengths become so small that the waveforms are aliased through the 9 discrete sensors.

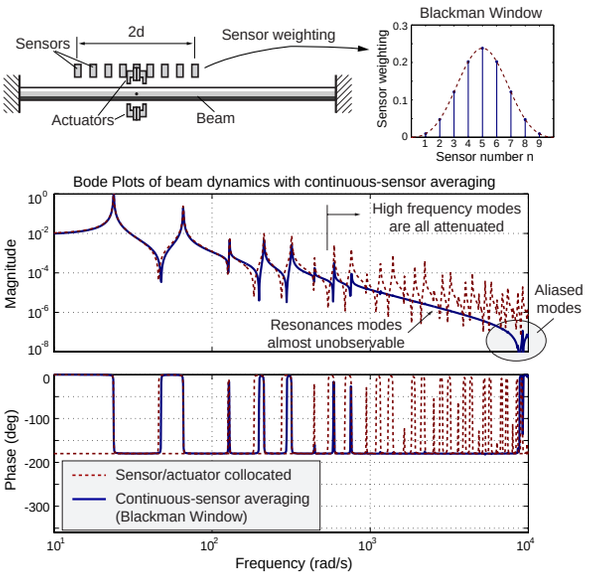

FIGURE 6: Theoretical beam model: Solid line shows 9-sensor averaging with a Blackman window. Dashed line shows a collocated beam model.

ACTUATOR AVERAGING

Actuator averaging is the dual to sensor averaging. Here, we use multiple actuators and apply the same force to each actuator. The resulting filtering effect is similar to sensor averaging. Actuator averaging attenuates the modal controllability, and sensor averaging attenuates the modal observability. Sensor averaging is easier to understand since it simply averages the vibration waveforms. Actuator averaging places actuators in a similar way such that certain resonance modes will not be excited, as can be interpreted from the concepts of modal forces. If we place one actuator at $z=z_0$, and apply force f from the actuator, the resulting nth modal force can be calculated by:

$$N_n = \int_0^L f(z)\phi_n(z)dz = \int_0^L f\delta(z_0)\phi_n(z)dz = f\phi_n(z_0) \quad (11)$$

We then place two actuators set apart by $2d$, and apply the same control forces $f/2$ to each actuator. With actuators located at $z_1=(z_0-d)$ and $z_2=(z_0+d)$, the averaged modal force is given by

$$N_n = \frac{f}{2}\left(\phi_n(z_1)+\phi_n(z_2)\right) = f\phi_n(z_0)\cos k_n d \quad (12)$$

By comparing Eq. 11 and Eq. 12; we can see that actuator averaging creates a modal gain of $\cos k_n d$ in a dual fashion to the sensor averaging.

Similar to 3-sensor averaging, by using 3 actuators, and assigning the force distribution as $f/4$ at $z=z_1$ and $z=z_2$, and $f/2$ at $z=z_0$, we can also create a cosine notch filter without phase change. Finally, we can extend our results to using many actuators, in dual to the multi-sensor case shown in Fig. 6.

Combination of Sensor/Actuator Averaging

In the ideal case, sensor averaging and actuator averaging will be used together. The resulting modal gain is the multiplication of both averaging effects. For beams, using two sensors set apart by $2d_s$ and two actuators set apart by $2d_a$, the filter gain of each mode becomes $\cos k_n d_s \cdot \cos k_n d_a$. The distances d_s and d_a can be arranged to meet the system's requirements and result in a broader overall notch.

EXPERIMENTAL RESULTS

In this section, we show the experimental results of magnetic suspension of a tubular beam. The experimental setup is shown in Fig. 1. The details of the sensor dynamics, actuator dynamics, and the controller design are presented in [7,8,9]. The experimental results shown here focus on the suspension of a single point of the beam to demonstrate the effectiveness of the proposed averaging methods. We used 4 such suspensions to successfully suspend the beam freely by independently controlling 4 points along the beam.

Experiment with 2-Sensor Averaging

We clamp the beam at both ends, support the beam weight by two strings, and place one actuator between two sensors to control the beam at one point at z=1.12 m. At first, we place sensors and the actuator in close proximity to simulate a collocated sensor/actuator pair. We are almost able to stabilize the system locally, except there is a limit cycle vibration at 1100 rad/s.

We pull the sensors apart to implement sensor averaging and eliminate the limit cycle. Specifically, the sensors are placed ±0.15 m from the actuator at z=1.12 m. Fig. 7 shows the experimental setup and the measured loop transfer function with a slow-rollup lead compensator. Sensor averaging shows an improvement of the gain margin within a frequency range from 700 to 1500 rad/s where the phase is below -180°. Thus we are able to stabilize the system and avoid the 1100 rad/s limit cycle. The modal observability becomes 180° out of phase after the cosine notch zero as predicted by the theoretical analysis.

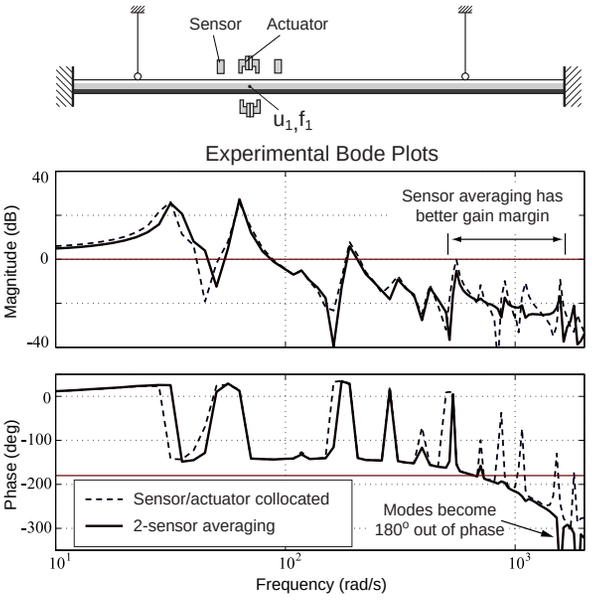

FIGURE 7: Experimental setup and Bode plots of loop transfer function by using 2-sensor averaging. Dashed line shows the collocated sensor/actuator experiment for comparison.

Experiment with 3-Sensor Averaging

To verify the proposed idea of a 3-sensor arrangement, we use 3 sensors and 2 actuators. Specifically, the sensors are placed ±0.15 m from each other about a center at z=1.12 m. The two actuators are placed closely to the sensor at the center. Fig. 8 shows the experimental setup and the measured loop transfer function. Notice that the modal observability stays in phase after the cosine notch zero.

Experiment with 2-Actuator Averaging

To verify the effectiveness of the proposed actuator averaging, we use 1 sensor and 2 actuators to implement this experiment. Specifically, the sensor is placed at z=1.12 m, and the actuators are placed ±0.17 m from the sensor. Fig. 9 shows the experimental setup and the measured loop transfer function. Notice the similarity between this setup and 2-sensor averaging.

Experiment with Both Sensor/Actuator Averaging

We successfully suspend a free-free beam by 8 sensors and 8 actuators. We apply both 2-sensor averaging and 2-actuator averaging to control 4 points along the beam independently. The sensor averaging is designed to

attenuate resonance modes in the vicinity of 160 Hz, and the actuator averaging is designed for 800 Hz. Our experiment shows the system is robustly stable for varying boundary conditions, including hinged, clamped, and free boundaries.

SUMMARY

This paper presents the novel results of sensor averaging and actuator averaging methods for vibration control of flexible structures. This method takes the advantage that the relations between resonance frequencies and wavelengths depend on structural properties and can be calculated. Therefore we can place sensors and actuators based on the wavelengths of undesired modes, and attenuate these resonance modes to improve the gain margin. Sensor averaging attenuates the modal observability, and actuator averaging attenuates the modal controllability. This averaging method is mathematically proved and experimentally verified. It creates a modal attenuation for undesired resonance modes without adversely affecting the phase. The resulting modal gain is independent of sensor/actuator pair locations, structural lengths and boundary conditions. This method is thus applicable to a wide range of structural control problems.

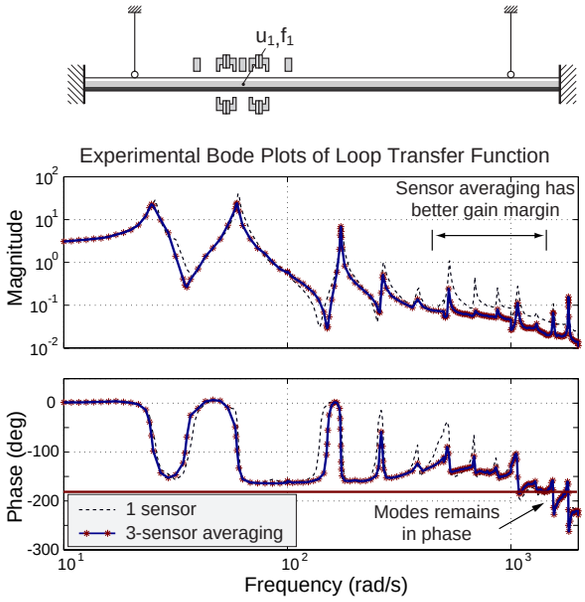

FIGURE 8: Experimental setup and Bode plots of loop transfer function by using 3-sensor averaging. The phase remains unchanged above the notch. Dashed line is measured with 1 sensor for comparison.

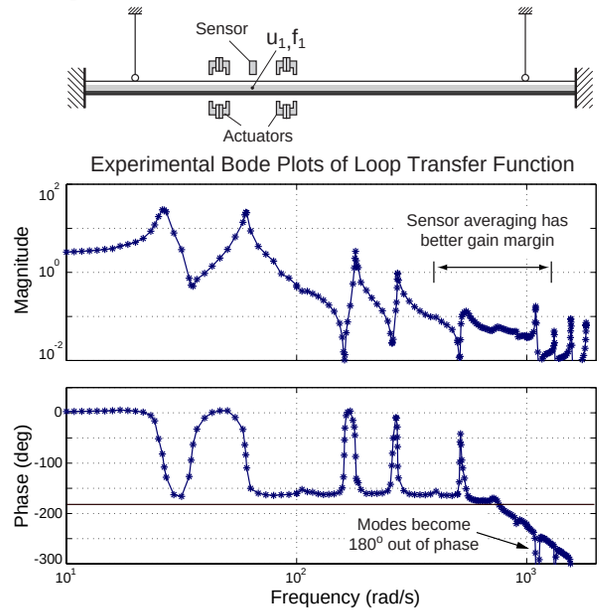

FIGURE 9: Experimental setup and Bode plots of loop transfer function by using 2-actuator averaging.

ACKNOWLEDGEMENT

This work is supported by the National Science Foundation under the grant award No. DMI-9700973.

REFERENCES

1. Y. Oshinoya, and T. Shimogo, Electro-magnetic Levitation Control of an Elastic Plate, Proc. of Maglev '89: 435-440, 1989.
2. H. Hayasiya, H. Ohsaki, and E. .Masada, Magnetic Levitation Control of Elastic Steel Plate for Steel Making Process, Proc. of ICEE '95, 1995.
3. American Metal Handle, Vulcan Dr., Birmingham, AL, USA.
4. L. Meirovitch, Elements of Vibration Analysis, McGraw-Hill, 2nd edition, 1986.
5. L. Meirovitch, The Implementation of Modal Filters for Control of Structures, J. of Guidance Control and Dynamics, 8(6): 707-716, 1985.
6. S. A. Collins, D. W. Miller, and A. H. von Flotow, Distributed Sensors as Spatial Filters in Active Structural Control, J. of Sound and Vibration, 173(4): 471-501, 1994.
7. M. C. Weng, and D. L. Trumper, A Design Method for Magnetic Suspension and Vibration Control of Levitated Beams for Noncontact Processing, Proc. of the 5th Int. Symp. of Magnetic Suspension Technologies, Dec. 1999.
8. D. L. Trumper, M. C. Weng, and R. J. Ritter, Magnetic Suspension and Vibration Control of Beams for Non-contact Processing, Proc. of the IEEE CCA-CACSD '99, pp. 551-557, 1999.
9. M. C. Weng, Magnetic Suspension and Vibration Control of Flexible Structures for Non-contact Processing, Ph.D. Thesis, Dept. of Mech. Eng., MIT, Feb. 2000.